Environmental and Experimental Botany 147 (2018) 95–103

Contents lists available at ScienceDirect

Environmental and Experimental Botany

journal homepage: www.elsevier.com/locate/envexpbot

Global warming interacts with ocean acidification to alter PSII function and protection in the diatom *Thalassiosira weissflogii*

Guang Gao[a,c], Qi Shi[b], Zhiguang Xu[a], Juntian Xu[c], Douglas A. Campbell[d], Hongyan Wu[a,b,*]

[a] College of Life Science, Ludong University, Yantai 264025, China
[b] Hubei Provincial Cooperative Innovation Center of Industrial Fermentation, Hubei University of Technology, Wuhan 430068, China
[c] Marine Resources Development Institute of Jiangsu, Huaihai Institute of Technology, Lianyungang 222005, China
[d] Biology Department, Mount Allison University, Sackville, New Brunswick E4L 1G7, Canada

ARTICLE INFO

Keywords:
Diatom
Nonphotochemical quenching
Ocean acidification
Warming
Photoprotection
Photoinactivation

ABSTRACT

Diatoms, as important contributors to aquatic primary production, are critical to the global carbon cycle. They tend to dominate phytoplankton communities experiencing rapid changes of underwater light. However, little is known regarding how climate change impacts diatoms' capacity in coping with variable light environments. Here we grew a globally abundant diatom *T. weissflogii,* under two levels of temperature (18, 24 °C) and pCO_2 (400, 1000 µatm), and then treated it with a light challenge to understand the combined effects of ocean warming and acidification on its exploitation of variable light environments. The higher temperature increased the photoinactivation rate at 400 µatm pCO_2 and the higher pCO_2 alleviated the negative effect of the higher temperature on PSII photoinactivation. Temperature did not affect the PsbA removal rate, but higher pCO_2 stimulated PsbA removal. Photoinactivation outran repair, leading to decreased maximum photochemical yield in PSII. The higher pCO_2 induced high sustained phase of nonphotochemical quenching when cells were less photoinhibited. The high light exposure induced the activity of both superoxide dismutase (SOD) and catalase (CAT) and the higher temperature stimulated them further, with insignificant effect of pCO_2. Our findings suggest that ocean warming, ocean acidification and high light exposure would interact on PSII function and protection, and combination of these three environmental factors would lead to a reduced PSII activity in *T. weissflogii*. This study provides helpful insight into how climate change variables combined with local stressor impact diatoms' photosynthetic physiology.

1. Introduction

Marine diatoms account for approximately 20% of total global primary production, through 35% of the primary productivity in the oligotrophic oceans and 75% of primary productivity in the coastal zone and other nutrient-rich systems (Nelson et al., 1995; Field et al., 1998; Falkowski, 2012). Marine diatoms often dominate the phytoplankton assemblage in areas with high water mixing (Macintyre et al., 2000), where they have to cope with rapid fluctuations of underwater light environment. Depending upon the depth of the upper mixed layer and the intensity of water mixing, diatoms may experience transient excess light that can produce oxidative stress and thus harm photosynthesis, leading to net photoinactivation (Dubinsky et al., 2009; Wu et al., 2012a; Xu et al., 2016). Diatoms have developed interacting strategies to combat the potentially damaging effects of excess light. Cells can repair damaged PSII by replacing photo-damaged proteins in PSII with newly synthesized subunits (Nixon et al., 2010; Komenda et al., 2012). If the rate of repair does not keep up with the rate of photoinactivation, the PSII pool suffers net photoinactivation, resulting ultimately in a decrease in photosynthetic quantum yield (Murata et al., 2007; Wu et al., 2012a). Compared to other marine phytoplankton taxa, marine diatoms have distinctive clearance patterns for the PsbA (D1), and PsbD (D2) PSII subunits and also a lower intrinsic susceptibility to photoinactivation of PSII upon elevated light levels (Six et al., 2009; Key et al., 2010; McCarthy et al., 2012). Another important strategy of diatoms to cope with a sudden increase in irradiance is non-photochemical quenching (NPQ) of captured excitation which in diatoms is dominated by one or more mechanisms activated by the *trans*-thylakoid proton gradient triggering the xanthophyll cycle (Lavaud et al., 2004; Lavaud and Lepetit, 2013). In parallel excessive light exposure can increase the formation of reactive oxygen species (ROS), impairing PSII repair (Nishiyama et al., 2006; Nishiyama and Murata, 2014) and thereby inhibiting photosynthesis (van de Poll et al., 2005). Diatoms have evolved an elaborate antioxidant network to scavenge ROS, for

* Corresponding author.
E-mail address: why-z-z@hotmail.com (H. Wu).

https://doi.org/10.1016/j.envexpbot.2017.11.014
Received 30 October 2017; Received in revised form 25 November 2017; Accepted 25 November 2017

Table 1
Parameters of the seawater carbonate system in different cultures. DIC = dissolved inorganic carbon, TA = total alkalinity. Data are the means ± SE (n = 4). Different superscript letters represent significant differences ($P < 0.05$) among cultures.

Species	Temperature (°C)	pCO_2 (μatm)	pH_{NBS}	DIC (μmol kg^{-1})	HCO_3^- (μmol kg^{-1})	CO_3^{2-} (μmol kg^{-1})	CO_2 (μmol kg^{-1})	TA (μmol kg^{-1})
T. weisflogii	18	381 ± 21^a	8.21 ± 0.02^b	2153 ± 92^a	1943 ± 82^a	197 ± 12^c	13.0 ± 0.7^a	2440 ± 103^a
		978 ± 45^b	7.86 ± 0.01^a	2331 ± 70^b	2200 ± 66^b	98 ± 4^a	33.4 ± 1.6^c	2452 ± 71^a
	24	384 ± 23^a	8.22 ± 0.02^b	2135 ± 46^a	1887 ± 47^a	237 ± 6^d	11.1 ± 0.7^a	2480 ± 43^a
		76 ± 30^b	7.87 ± 0.01^a	2293 ± 60^b	2144 ± 55^b	120 ± 4^b	28.3 ± 0.9^b	2450 ± 63^a

instance, the superoxide radical is converted enzymatically to H_2O_2 by superoxide dismutase (SOD), which is subsequently neutralized to H_2O by catalase (CAT) (Drábková et al., 2007; Li et al., 2015; Smerilli et al., 2017).

The global sea surface temperature increased at a rate of 0.121–0.124 °C per decade based on *in situ* data records from 1979 to 2012 (IPCC, 2013). The global ocean will continue to warm during the 21 st century and the global mean sea surface temperature has been predicted to increase by 1.18–6.48 °C by the end of the 21st century (Meehl et al., 2007). The anthropogenically driven temperature rise will exert considerable direct and indirect influences on marine phytoplankton. The photosynthetic carbon fixation and biomass of marine phytoplankton decrease at warmer sea surface temperatures, which could be attributed to the strengthened stratification and thus decreased nutrient supply from deeper waters (Behrenfeld et al., 2006; Poll et al., 2013; Gao et al., 2017a). The strengthened stratification could enhance average light exposure by trapping cells higher in the photic zone and thus reduce PSII function of diatoms (Gao et al., 2009; Wu et al., 2012b) or marine primary productivity (Gao et al., 2012, 2017b) when combined with higher pCO_2. Meanwhile, elevated temperature can also affect the photosynthesis and growth of algae directly. For instance, an increase of temperature from 12 °C to 18 °C increased the growth rate in *T. pseudonana* (Wu et al., 2012a); a 3 °C of seawater warming also stimulated the biomass and photosynthetic carbon fixation of phytoplankton in South China Sea (Gao et al., 2017b).

The atmospheric CO_2 level has increased from 280 ppm in the late 1700 s to 407 ppm in July of 2017 (NOAA, 2017), due largely to the burning of fossil fuels and change of land use (IPCC, 2013). The increase of atmospheric CO_2 level (ppm) inevitably leads to the rise of CO_2 pressure (μatm) in seawater. The ocean has so far absorbed about 30% of the anthropogenic CO_2 emitted to the air, leading to a decrease of 0.1 unit pH in the surface ocean since the beginning of the industrial era (IPCC, 2013). The decline in seawater pH, together with associated changes in seawater carbonate system, is termed ocean acidification. Based on the Representative Concentration Pathway (RCP) 8.5 projection, mean surface ocean pH will further decrease by 0.30–0.32 units by 2100 (IPCC, 2013). The rapidly changing seawater carbon chemistry climate will differentially influence marine organism performances (Hoeghguldberg and Bruno, 2010; Mostofa, 2016), including the response of algae to the light environment (Sobrino et al., 2008; McCarthy et al., 2012; Jin et al., 2016). For instance, *T. pseudonana* growing under elevated pCO_2 demonstrated an augmented susceptibility to PSII photoinactivation compared to those under ambient pCO_2 (Sobrino et al., 2008; McCarthy et al., 2012). In contrast, elevated pCO_2 did not affect the susceptibility of *Emiliania huxleyi* to PSII photoinactivation caused by PAR (McCarthy et al., 2012) and decreased susceptibility of *Nannochloropsis* to UVR due to the enhancement of cellular repair (Sobrino et al., 2005). Furthermore, Li and Campbell (2013) found the effect of pCO_2 on photoinactivation interacted with growth light intensity. *T. pseudonana* cultured under 750 μatm pCO_2 showed less photoinhibition for photosynthesis when growth light level was less than 300 μmol photons m^{-2} s^{-1} compared to that under ambient pCO_2 but equal or even greater photoinhibition for photosynthesis when growth light level was *c.* 380 μmol photons m^{-2} s^{-1} (Li and Campbell, 2013). In addition, Hoppe et al. (2015) reported that 1000 μatm pCO_2 decreased the light-use efficiency in an Antarctic diatom *Chaetoceros debilis* under dynamic rather than constant light.

Ocean warming and acidification do not incur in isolation; instead, they are approaching simultaneously. However, little is known regarding the combined, interacting effects of these two important global variables and the local stressor (high light) on photoinactivation, repair, and protection in phytoplankton. In this study we cultured a cosmopolitan diatom *T. weissflogii* under current and future temperature and pCO_2 conditions. We monitored the changes in photoinactivation, PsbA, NPQ, superoxide dismutase (SOD) and catalase (CAT), in cells treated with a light challenge, to understand how future ocean warming and acidification interact on the strong capacities of diatoms to exploit variable light.

2. Materials and methods

2.1. Culture conditions and seawater carbonate system

All experiments were conducted with cultures of one globally abundant diatom species (Leblanc et al., 2012), *Thalassiosira weissflogii* (CCMA102, ~11 μm), which was isolated from the Northern South China Sea. Cells were grown semi-continuously in f/2 medium (Guillard and Ryther, 1962), based on artificial seawater prepared according to Morel et al. (1979). We diluted the cultures by using pre-CO_2-equilibrated medium every 24 h, and maintained the density less than 10 μg chlorophyll *a* L^{-1}, so that the seawater carbonate chemistry parameters were stable (Table 1) with pH variations < 0.05 units. Two levels of pCO_2 (400, 1000 μatm) and temperature (18 °C, 24 °C) were imposed in the plant growth CO_2 chambers (HP 1000G-D, Ruihua, China). The 18 °C is seawater temperature of sampling sit. Cultures in the growth chamber were illuminated at 100 μmol photons m^{-2} s^{-1} provided by cool white fluorescent tubes with a 12 h: 12 h light: dark cycle. All cultures were grown through at least seven transfers of semi-continuous dilution to obtain steady growth rates under the given culture conditions to ensure full acclimation before use in subsequent experiments. There were four replicates under each treatment.

pH changes in the medium were determined with a pH meter (SevenMulti S40 K, Mettler-Toledo) which was calibrated with National Bureau of Standard (NBS) buffers of pH 7.0 and 10.0 (Sigma-Aldrich). DIC was measured by using a Shimadzu Total Organic Carbon Analyzer (TOC-5000A, Japan) and total alkalinity was measured by potentiomentric titration. Subsequently, other parameters of the carbonate system were derived with CO_2SYS software (Pierrot et al., 2006) based on the known values of DIC, pH, salinity, alkalinity and temperature.

2.2. Upward light shift and recovery experiment

Culture replicates were split into two flasks and one was supplemented with a final concentration of 500 μg mL^{-1} lincomycin to block chloroplast protein synthesis (Wu et al., 2012a), thereby inhibiting PSII repair (Tyystjärvi and Aro, 1996; Wu et al., 2012a). Both flasks were placed in the dark for 10 min to allow the lincomycin to exert its effect and then exposed to fluorescent lamps (Philips, 21 W) at an intensity of 800 μmol photons m^{-2} s^{-1} for 120 min. Samples were collected prior to the onset of high light (plotted as time 0) and then after 30, 60, 90,

and 120 min exposure for chlorophyll fluorescence analyses and also for protein immunoblotting. After the high-light treatment, the remaining culture was returned to their growth light of 100 μmol photons $m^{-2} s^{-1}$ for a 30-min recovery period followed by the final sampling and measurement.

2.3. Chlorophyll fluorescence measurement and parameterization

Chlorophyll fluorescence was determined using a portable pulse amplitude modulated fluorometer (WATER-PAM, Walz, Germany). At each sampling point, the samples were dark adapted for 5 min first to relax photosynthetic activity. The maximal efficiency ofPSII photochemistry was determined as the ratio of variable to maximal chlorophyll fluorescence (F_V/F_M), where $F_V = (F_M - F_0)$, F_M and F_0 were the maximal and minimal fluorescence yield, respectively, of a dark-adapted suspension. F_0 was measured by using modulated measuring light (< 0.1 μmol photons $m^{-2} s^{-1}$) and F_M was determined at a 0.5 s saturating pulse of 4000 μmol photons $m^{-2} s^{-1}$ in dark-adapted cells.

A sustained phase of NPQ, NPQs, which was induced over the course of the high-light treatment and persisted through the 5-min dark acclimation period just before measurement (Wu et al., 2012a), was estimated as:

$$NPQs = (F_{Mt0} - F_M)/F_M.$$

F_{Mt0} is the measurement of F_M from dark-acclimated cells, taken at time t_0 just before the start of high-light treatment. F_M is taken at each measurement time point after 5 min dark relaxation. By definition, NPQs thus starts from 0 at T_0, and increases if the cells accumulate a sustained phase of NPQ (Lavaud et al., 2004). NPQs reflects an inducible increase in the relaxation time for a fraction of NPQ, persisting beyond a 5-min dark period.

A functional absorption cross-section driving the photoinactivation of PSII (σ_i, $Å^2$ quanta^{-1}) was estimated by plotting a single phase exponential decay through a plot of F_V/F_M (Campbell and Tyystjärvi, 2012) versus the cumulative photons (quanta $Å^{-2}$) applied during the 800 μmol photons $m^{-2} s^{-1}$ light treatment. F_V/F_M values measured during the 800 μmol photons $m^{-2} s^{-1}$ light treatment were corrected for the effect of NPQs, prior to the curve fitting for estimation of σ_i, to separate photoinactivation of PSII from the influence of NPQs (Wu et al., 2012a). The correction for NPQs was applied by determining the amplitude of recovery (if any) in F_V/F_M in cells incubated with lincomycin, and transferred from the 800 μmol photons $m^{-2} s^{-1}$ light treatment back down to growth light of 100 μmol photons $m^{-2} s^{-1}$, for a 30-min recovery period. This recovery amplitude in the presence of lincomycin was attributed to relaxation of NPQs. Multiplying σ_i by the applied photons $Å^{-2} s^{-1}$ generates a rate constant for photoinactivation (k_{pi}, s^{-1}) for the particular applied light level (Kok, 1956). The apparent rate constant for PSII repair (K_{rec}, s^{-1}) was initially estimated according to Campbell and Tyystjärvi (2012).

2.4. SDS-PAGE analysis and western blot

At each sampling point cells were harvested on glass fiber filters (25 mm diameter, binder-free glass fiber, Whatman), which were immediately flash frozen in liquid nitrogen and stored at −80 °C until later protein analyses. Total proteins were extracted by two thawing/sonicating rounds in denaturing extraction buffer (Brown et al., 2008). The total protein concentration was determined using a Lowry protein assay kit (Bio-Rad DC Assay). Western blots were performed for PsbA, a core reaction center protein in Photosystem II. Two μg of total protein was loaded on a 6% to 12% acrylamide gel. Molar levels of PsbA (www.agrisera.se antibody AS05084; standard: AS01016S) were then determined with quantitative immunoblotting (Wu et al., 2011).

We estimated a rate constant for the clearance of PsbA protein by plotting fmol PsbA μg total protein^{-1}, for cells incubated under the 800 μmol photons $m^{-2} s^{-1}$ treatment in the presence of lincomycin to block the counteracting synthesis of PsbA through chloroplast translation. We fit this PsbA plot with a single-phase exponential decay over the period from 0 to 120 min of high-light incubation. This K_{PsbA} rate constant reflects the capacity for removal of PsbA protein from the PSII pool ($[PSII]_{active}$) (Wu et al., 2012a). The inactivated PSII pool ($[PSII]_{inactive}t_0$) at the start of the high light treatment was then estimated by using the K_{PsbA} as an input for $K_{recinact}$ according to Ni et al. (2017), relative to a starting $[PSII]_{active}$ of 100:

$$[PSII]_{active}t = \left\{ [PSII]_{active}t_0 \times \left(\frac{K_{recinact}}{K_{pi} + K_{recinact}} + \frac{K_{pi}}{K_{pi} + K_{recinact}} \times e^{-(K_{pi}+K_{recinact})\times t} \right) + [PSII]_{inactive}t_0 \times \frac{K_{recinact}}{K_{pi} + K_{recinact}} \times \left(1 - e^{-(K_{pi}+K_{recinact})\times t}\right) \right\},$$

where K_{pi} is the first-order rate constant for photoinactivation of PSII, s^{-1} (Kok, 1956); $K_{recinact}$ by definition is the first-order rate constant for recovery of photoinactivated PSII, allowing for initial pool of $[PSII]_{inactive}$ t_0, s^{-1}.

2.5. Assay of superoxide dismutase (SOD) and catalase (CAT) activity

At each sampling point, cells were collected onto a polycarbonate membrane (0.22 μm, Whatman) and washed into a 1 mL centrifuge tube with phosphate buffer (pH 7.6). The enzyme extractions were carried out in 0.6 mL phosphate buffer (pH 7.6) that contained 50 mM KH_2PO_4, 1 mM ethylenediaminetetraaceticacid (EDTA), 0.1% Triton X-100 and 1% (w/v) polyvinylpolypyrrolidone. After the homogenized extract was centrifuged at 12000*g* (4 °C) for 10 min, SOD and CAT activities were tested by using SOD and CAT Assay Kits (Nanjing Jiancheng Biological Engineering Company, China). One unit of SOD activity was defined as the amount of enzyme which resulted in a 50% inhibition of the rate of nitro-blue tetrazolium reduction at 560 nm (Wang and Wang, 2010). CAT activity was determined by measuring the initial rate of disappearance of H_2O_2 at 240 nm (Li et al., 2015).

2.6. Statistical analysis

Results are expressed as means of replicates ± standard error. Data were statistically analyzed using the software SPSS v.21. The data under every treatment conformed to a normal distribution (Shapiro-Wilk, $P > 0.05$) and the variances could be considered equal (Levene's test, $P > 0.05$). Two-way multivariate ANOVAs (MANOVAs) were conducted to assess the effects of temperature and pCO_2 on carbonate parameters in cultures. Tukey HSD was conducted for *post hoc* investigation. Repeated measures ANOVAs (RM-ANOVAs) were conducted to analyze the effect of exposure time on F_V/F_M, PsbA content, NPQs, SOD activity, and CAT activity. Bonferroni post-tests were conducted for *post hoc* investigation. Two-way MANOVAs were used to analyze the effects of temperature, pCO_2 and species on F_V/F_M, PsbA content, NPQs, SOD activity, and CAT activity in *T. weissflogii* at different exposure times. Two-way ANOVAs were used to analyze the effects of temperature, pCO_2 and species on photoinactivation rate constant, PsbA removal rate constant and $[PSII]_{active}t_0$ in *T. weissflogii*. Significance was determined at $P < 0.05$ for all tests.

3. Results

The carbonate system in the 1000 μatm pCO_2-grown cultures differed from that of 400 μatm pCO_2-grown cultures for both 18 °C and 24 °C (Table 1); DIC, HCO_3^- and CO_2 increased ($F_{(1,12)} > 86.248$, $P < 0.001$), CO_3^{2-} decreased ($F_{(1,12)} > 601.169$, $P < 0.001$) while total alkalinity was not significantly changed ($F_{(1,12)} < 0.193$, $P > 0.668$).

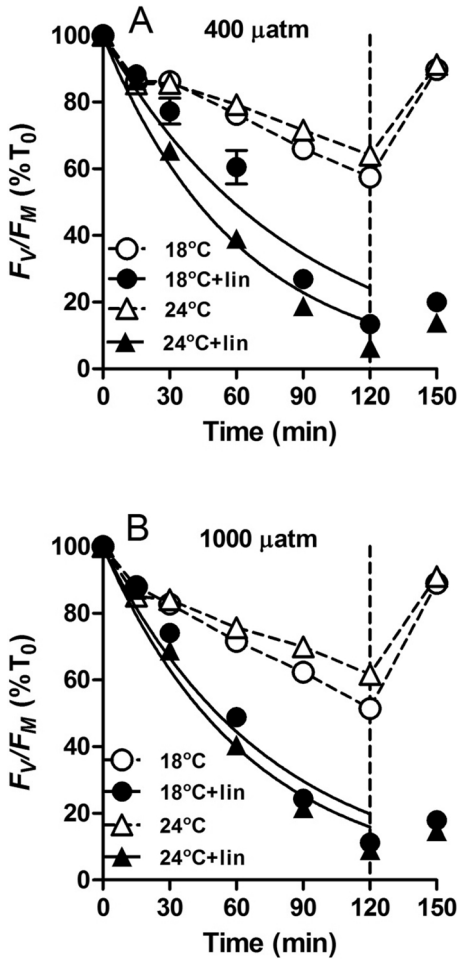

Fig. 1. Responses of PSII maximum photochemical yield (F_V/F_M) versus exposure time to high light in *T. weissflogii* (A, B) cultures treated with (black symbols) or without (white symbols) the chloroplast protein synthesis inhibitor lincomycin. Cells were grown under two levels of temperature (18, 24 °C) and pCO_2 (400, 1000 µatm) at the light intensity of 100 µmol photons $m^{-2} s^{-1}$, then exposed to 800 µmol photons $m^{-2} s^{-1}$high light for 120 min, and then allowed to recover at 100 µmol photons $m^{-2} s^{-1}$ for 30 min. The solid line shows the exponential decay fit of the F_V/F_M in the lincomycin-treated samples versus time. Data are the means ± SE (n = 4), most error bars within symbols.

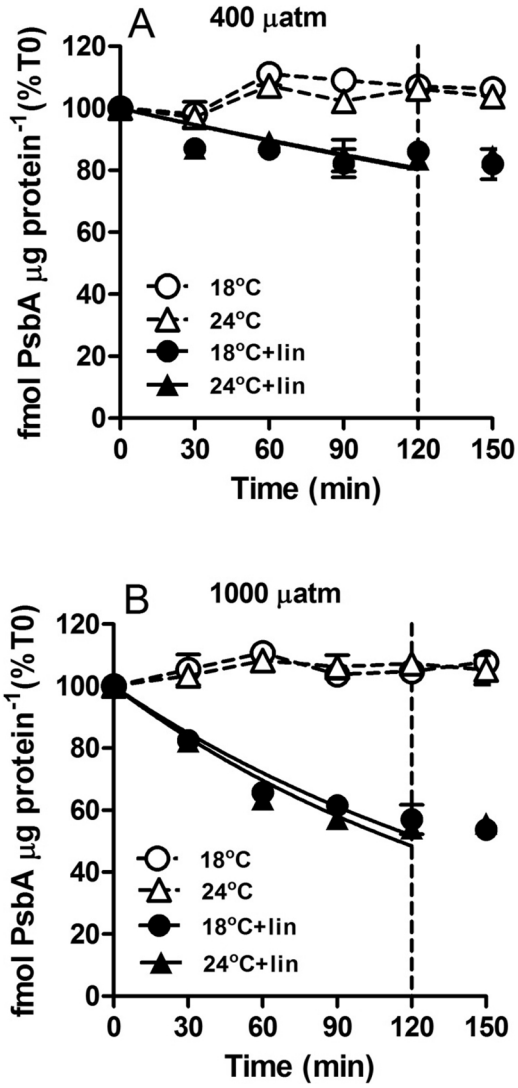

Fig. 2. Changes in PsbA protein content in *T. weissflogii* (A, B) cultures treated with (black symbols) or without (white symbols) the chloroplast protein synthesis inhibitor lincomycin. Cells were grown under two levels of temperature (18, 24 °C) and pCO_2 (400, 1000 µatm) at the light intensity of 100 µmol photons $m^{-2} s^{-1}$, then exposed to 800 µmol photons $m^{-2} s^{-1}$ high light for 120 min, and then allowed to recover at 100 µmol photons $m^{-2} s^{-1}$ for 30 min. The solid line shows the exponential decay fit of the PsbA content in the lincomycin-treated samples versus time. Data are the means ± SE (n = 4).

PSII function (F_V/F_M) in *T. weissflogii* grown under all conditions decreased with exposure time when the cells were shifted from low light (100 µmol photons $m^{-2} s^{-1}$) to high light (800 µmol photons $m^{-2} s^{-1}$) (black symbols, Fig. 1, $F_{(5,60)} = 1795.297$, $P < 0.001$), even when PSII repair was active (white symbols, Fig. 1, $F_{(5,60)} = 771.711$, $P < 0.001$). At the end of 120 min exposure, the higher temperature increased the final F_V/F_M ($F_{(1,12)} = 31.065$, $P < 0.001$) in *T. weissflogii*. When lincomycin was added to block the PSII repair cycle (black symbols), a more severe decline was detected in F_V/F_M under each condition ($F_{(1,24)} = 2449.419$, $P < 0.001$). After the recovery at low light for 30 min, the F_V/F_M rose to 89.0–91.3% of the initial value ($F_{(1,12)} = 697.178$, $P < 0.001$) in the absence of lincomycin and neither temperature nor pCO_2 affected the final F_V/F_M.

After shifting to high light, the content of PsbA in cells with ongoing PSII repair (white symbols) increased slightly after 120 min exposure ($F_{(1,12)} = 25.652$, $P < 0.001$, Fig. 2) but temperature ($F_{(1,12)} = 0.123$, $P = 0.732$) or pCO_2 ($F_{(1,12)} = 0.063$, $P = 0.806$) did not change the content of PsbA. The addition of lincomycin resulted in a noticeable decrease of PsbA during the high light exposure ($F_{(1,24)} = 37.303$, $P < 0.001$). The shift to low light for 30 min did not affect PsbA content of *T. weissflogii* regardless of presence ($F_{(1,12)} = 0.110$, $P = 0.746$) or absence of lincomycin ($F_{(1,12)} = 0.336$, $P = 0.573$).

The photoinactivation rate constant (K_{pi}) in *T. weissflogii* (Fig. 3A) grown at different conditions was estimated by fitting a single-phase exponential decay to the F_V/F_M of the lincomycin-treated samples (Fig. 1). Temperature and pCO_2 interacted ($F_{(1,12)} = 15.703$, $P = 0.002$) on K_{pi} and temperature had a main effect ($F_{(1,12)} = 72.262$, $P < 0.001$). The higher temperature increased K_{pi} at 400 µatm pCO_2 by 29.7% but did not affect it at 1000 µatm pCO_2, indicating that higher pCO_2 could alleviate the negative effect of high temperature on photosystem activity.

The PsbA removal rate constants (K_{PsbA}) in *T. weissflogii* cultured with varying temperature and pCO_2 treatments were also investigated (Fig. 3B). Temperature did not significantly affect the K_{PsbA} ($F_{(1,12)} = 0.700$, $P = 0.419$) but 1000 µatm pCO_2 significantly increased ($F_{(1,12)} = 167.390$, $P < 0.001$) compared to 400 µatm pCO_2.

The NPQs increased with high light exposure time ($F_{(5,60)} = 135.732$, $P < 0.001$, Fig. 4). After 120 min exposure, neither temperature ($F_{(1,12)} = 0.968$, $P = 0.345$) nor pCO_2 ($F_{(1,12)} = 1.599$, $P = 0.230$) affected NPQs. The addition of lincomycin led to larger increases in NPQs ($F_{(1,24)} = 172.394$, $P < 0.001$), concomitant with larger drops in F_V/F_M (Fig. 1) and losses of PsbA protein (Fig. 2). During

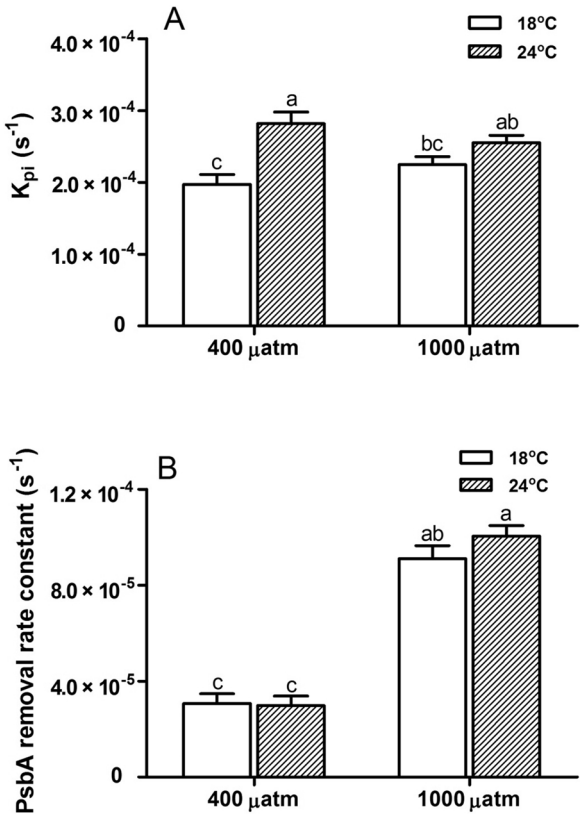

Fig. 3. Photoinactivation rate constant (K_{pi}, s^{-1}) (A) and PsbA removal rate constant (K_{PsbA}, s^{-1}) (B) in *T. weissflogii* (A, B) grown under two levels of temperature (18, 24 °C) and pCO_2 (400, 1000 µatm) with the light intensity of 100 µmol photons m^{-2} s^{-1}. Rate constants were estimated from samples taken during 120 min of exposure to 800 µmol photons m^{-2} s^{-1} light intensity. Data are the means ± SE (n = 4). Different superscript letters indicate significance differences (Tukey HSD, $P < 0.05$) in K_{pi} or in K_{PsbA} among treatments.

subsequent 30 min of low light exposure, the NPQs without lincomycin decreased to nearly zero but did not relax in the presence of lincomycin. Given the unfolding complexities of NPQ in diatoms (Lavaud and Lepetit, 2013; Giovagnetti and Ruban, 2017), we are not assigning a mechanistic interpretation to this NPQs. NPQs does accumulate and subsequently relaxed when chloroplastic protein synthesis was active under low light, but as we have previously observed the relaxation is blocked in the absence of chloroplastic protein synthesis (Wu et al., 2011, 2012a).

To investigate the potential connections among thermal dissipation, photoinactivation and PsbA clearance, the correlation between NPQs induction and K_{pi}/K_{PsbA} under various growth conditions was analyzed (Fig. 5A). Compared to 400 µatm CO_2 (white symbols), diatoms under 1000 µatm CO_2 (black symbols) induced NPQs at a lower ratio of K_{pi} to K_{PsbA} ($F_{(1,12)} = 4.877$, $P = 0.047$). In Fig. 5B we plotted the K_{PsbA} versus K_{pi}, for cells treated with lincomycin to block counteracting repair processes. Photoinactivation consistently outruns the short term removal of PsbA upon the upward light shift. Although 1000 µatm CO_2 (black symbols) greatly improved K_{PsbA} ($F_{(1,12)} = 350.801$, $P < 0.001$), it still lagged behind K_{pi}. The plot of the apparent functional PSII repair rate constant (K_{rec}) versus K_{PsbA} (Fig. 5C) showed that functional recovery of PSII greatly exceeded K_{PsbA}. The stimulation of higher CO_2 (black symbols) on removal of PsbA was not enough to catch up with apparent K_{rec}. Since the apparent K_{rec} is obtained by assuming that at t_0 of the time course all PSII is in the form $[PSII]_{active}$, it leads to an overestimation of the actual K_{rec} if cells contain an initial pool of $[PSII]_{inactive}t_0$, the substrate for the recovery process. We thus took measured K_{PsbA} as a proxy for the actual capacity for sustained K_{rec} and used it to estimate the number of $[PSII]_{inactive}t_0$ at the start of high

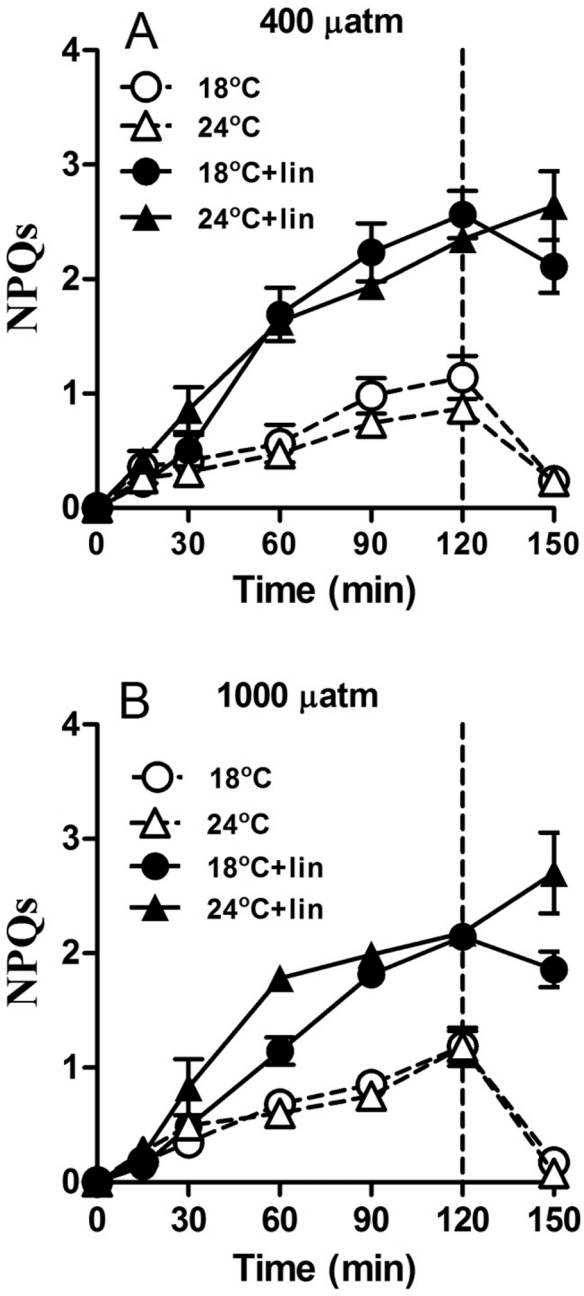

Fig. 4. Responses of sustained NPQ (NPQs) versus exposure time of high light in *T. weissflogii* (A, B) cultures treated with (black symbols) or without (white symbols) the chloroplast protein synthesis inhibitor lincomycin. Cells grown under two levels of temperature (18, 24 °C) and pCO_2 (400, 1000 µatm) with the light intensity of 100 µmol photons m^{-2} s^{-1}were exposed to 800 µmol photons m^{-2} s^{-1} high light for 120 min, and then allowed to recover at 100 µmol photons m^{-2} s^{-1} for 30 min. Data are the means ± SE (n = 4).

light exposure, relative to a starting $[PSII]_{active}$ of 100 (Ni et al., 2017).

As shown in Fig. 6, cells contain initial pools of $[PSII]_{inactive}$, allowing us to reconcile the apparent functional K_{rec} exceeding the measured K_{rec}. Increased temperature significantly increased it in *T. weissflogii* under 400 µatm pCO_2 ($F_{(1,12)} = 43.099$, $P < 0.001$). Cells grown at 1000 µatm pCO_2 contained much lower $[PSII]_{inactive}$ t_0 as compared to that under 400 µatm pCO_2 ($F_{(1,12)} = 333.275$, $P < 0.001$), showing an initial 1:1 ratio of $[PSII]_{inactive}$ t_0 to $[PSII]_{active}$ t_0.

After the shift to high light, the activity of superoxide dismutase (SOD) increased with exposure time for all culture conditions ($F_{(5,60)} = 11.096$, $P < 0.001$, Fig. 7). After 120 min exposure, the

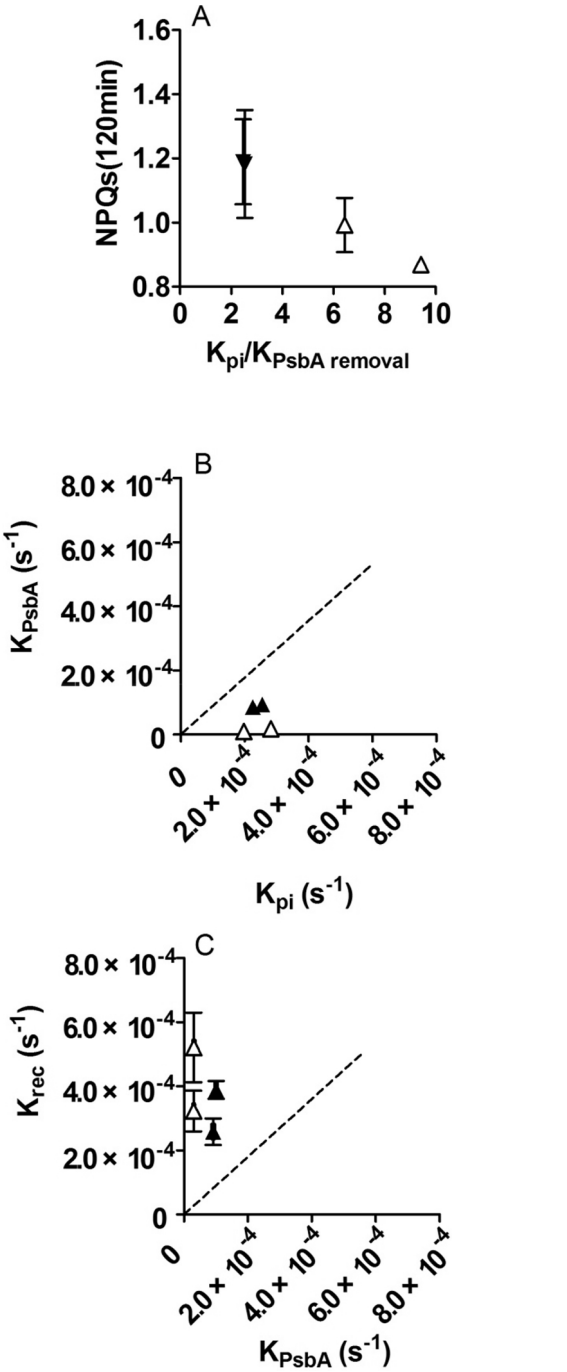

Fig. 5. Accumulated NPQs plotted versus the ratio of the photoinactivation rate constant for PSII (K_{pi}) to the PsbA removal rate constant (K_{PsbA}) (A), correlation of K_{PsbA} (s^{-1}) and K_{pi} (s^{-1}) (B), and correlation of apparent PSII repair rate constant (K_{rec}, s^{-1}) and K_{pi} (s^{-1}) (C) for *T. weissflogii* cells grown under two levels of temperature (18, 24 °C) and pCO_2 (400 µatm, white symbols; 1000 µatm, black symbols). NPQs and rate constants were estimated from samples taken during 120 min exposure to 800 µmol photons m^{-2} s^{-1} light. Dotted line indicates 1:1 ratio. Data are the means ± SE (n = 4).

higher temperature increased SOD activity in *T. weissflogii* ($F_{(1,12)}$ = 10.447, P = 0.007), with insignificant effect of pCO_2 ($F_{(1,12)}$ = 2.386, P = 0.148). The 30 min low light recovery period did not statistically decrease the activity of SOD ($F_{(1,12)}$ = 0.836, P = 0.378).

Upon the shift to high light at 18 °C, the catalase (CAT) activity did not change during first 15 min but then gradually increased ($F_{(1,12)}$ = 24.365, P < 0.001, Fig. 8). After 120 min exposure, the higher temperature increased CAT activity in *T. weissflogii*

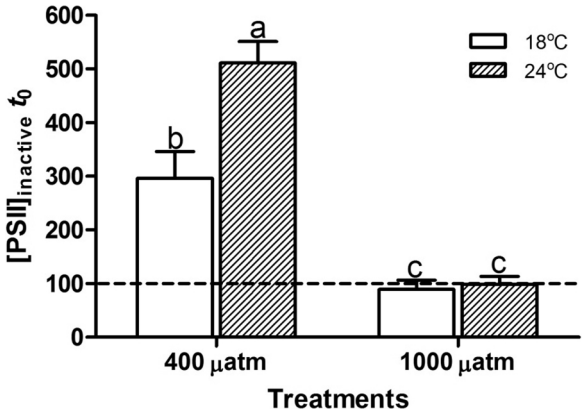

Fig. 6. The number of inactivated PSII complex in *T. weissflogii* grown under two levels of temperature (18, 24 °C) and pCO_2 (400, 1000 µatm), prior to the start of the high light exposure. The number of $[PSII]_{inactive}t_0$ was estimated relative to a starting active PSII content of 100 as indicated by the dashed line. n = 4, ± SE. Different superscript letters indicate significance differences (Tukey HSD, P < 0.05) in $[PSII]_{inactive}t_0$ among treatments.

($F_{(1,12)}$ = 71.362, P < 0.001) while the higher pCO_2 did not affect it ($F_{(1,12)}$ = 0.306, P = 0.590).

4. Discussion

4.1. Combined effects of light, temperature and pCO_2 on photoinactivation and repair

When cells were transferred from growth light to higher light, the PSII quantum yield (F_V/F_M) in cells grown at all conditions decreased with time, indicating the inhibitive effect of high light on photosynthesis. Turnover of PsbA protein is required for PSII repair and restoration of PSII photochemical activity (Aro et al., 1993; Edelman and Mattoo, 2008; Komenda et al., 2012). We found that the total pool of PsbA protein increased in *T. weissflogii* when the repair cycle was active, even though the F_V/F_M decreased. This indicates that maintenance of PsbA protein pool did not alone suffice for these cells to maintain their pool of active PSII, and that diatom cells can accumulate subpools of PsbA beyond their pools of active PSII. When lincomycin—an inhibitor for chloroplast protein synthesis—was added, a larger decline was found in both F_V/F_M and in pools of PsbA, showing the critical role of PsbA synthesis in repair and maintenance of active PSII.

Cells grown at the higher temperature suffered a higher photoinactivation rate constant when pCO_2 is 400 µatm. Temperature exerts a substantial influence on most cellular processes, such as enzymatic reactions. In general, activity of PSII increases with temperature for diatoms until an optimum is reached (Morris and Kromkamp, 2003; Yun et al., 2010; Wu et al., 2012b). The summer seawater temperature in northern South China Sea where *T. weissflogii* was isolated could be up to 30 °C (Jin et al., 2016; Gao et al., 2017b), indicating the higher temperature is within the range of natural grow in *T. weissflogii*. The contrary finding in this study may be attributed to that the combined effect of high temperature and high light, considering that PSII function is indeed one of the most thermosensitive components of photosynthetic process (Mathur et al., 2014). This hypothesis is supported by the result that the higher temperature did not affect the activity of PSII when cells were transferred to the low light condition.

On the other hand, the high temperature did not significantly increase photoinactivation rate when cells were grown at 1000 µatm pCO_2, indicating that the negative effect of the higher temperature upon PSII activity was somewhat alleviated by higher pCO_2 in the present study. This could be attributed to the accelerated net clearance of PsbA from a pool of photoinactivated PSII centers at the higher pCO_2. Increased CO_2 could usually down-regulate algal CCMs and save the

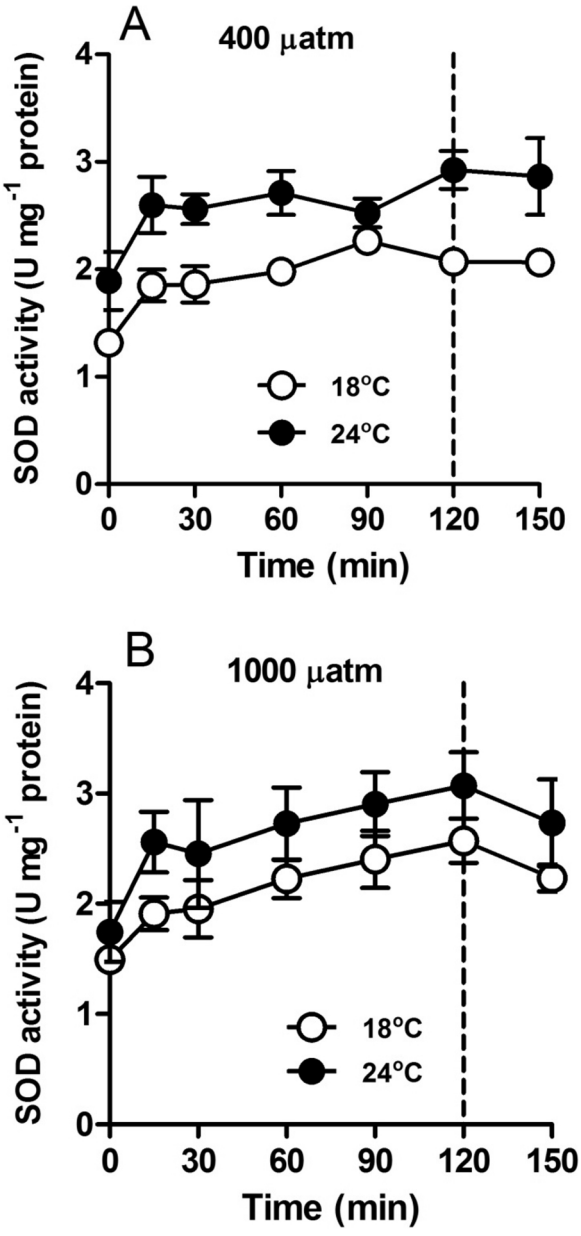

Fig. 7. Changes in superoxide dismutase (SOD) activity in *T. weissflogii* (A, B). Cells were grown under two levels of temperature (18, 24 °C) and pCO_2 (400, 1000 μatm) under a light intensity of 100 μmol photons $m^{-2} s^{-1}$, then exposed to 800 μmol photons $m^{-2} s^{-1}$ high light for 120 min, and then allowed to recover at 100 μmol photons $m^{-2} s^{-1}$ for 30 min. Data are the means ± SE (n = 4).

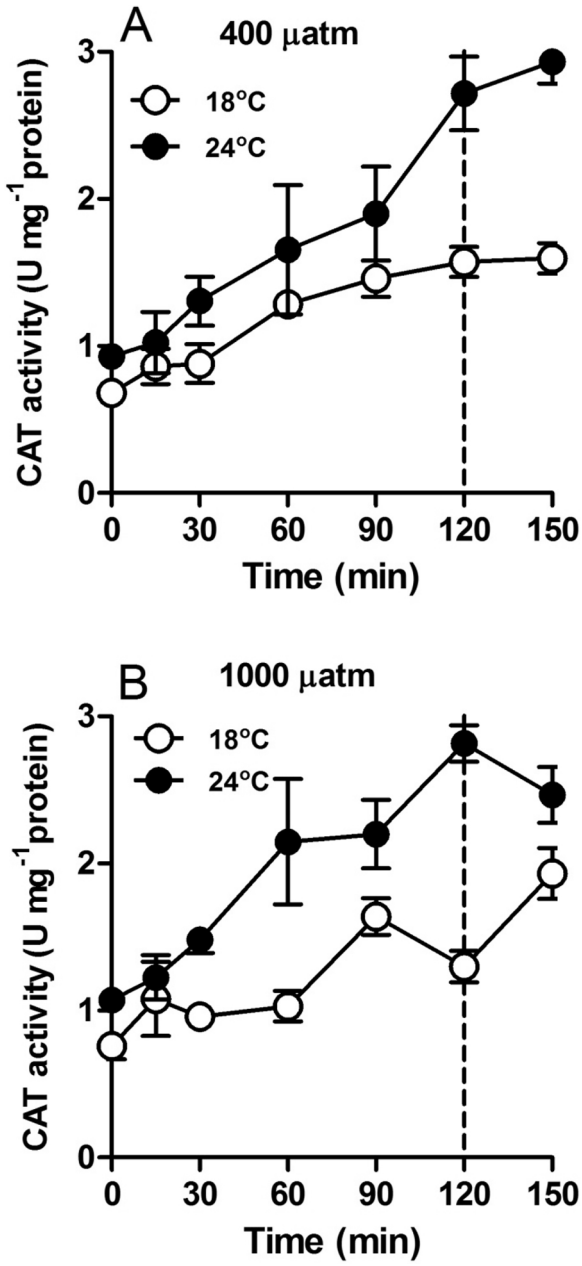

Fig. 8. Changes in catalase (CAT) activity in *T. weissflogii* (A, B). Cells grown under two levels of temperature (18, 24 °C) and pCO_2 (400, 1000 μatm) with the light intensity of 100 μmol photons $m^{-2} s^{-1}$ were exposed to 800 μmol photons $m^{-2} s^{-1}$ high light for 120 min, and then allowed to recover at 100 μmol photons $m^{-2} s^{-1}$ for 30 min. Data are the means ± SE (n = 4).

energy to operate inorganic carbon acquisition (Gao et al., 2012; Wu et al., 2012b; Xu et al., 2017). Additionally, our recent study with *T. pseudonana* showed that PSI activity in cells grown under high pCO_2 could be enhanced to support an increase in ATP synthesis by cyclic electron transfer (Shi et al., 2016). The proteolytic removal of PsbA subunits by the membrane-bound FtsH protease requires ATP (Nagao et al., 2012; Campbell et al., 2013), thus the saved or extra ATP generation might support faster removal of PsbA under high pCO_2 conditions. Although growth under high pCO_2 stimulated the removal of PsbA, it still lags behind the functional photoinactivation of PSII under high light, indicating that cells are building up a growing pool of inactivated PsbA during the high light treatment. However, cells at the start of high light exposure already contained an initial pool of $[PSII]_{inactive}$ (Fig. 6) which can serve as a substrate for short-term recovery of the $[PSII]_{active}$ pool, even when clearance of PsbA lags behind photoinactivation. Under high pCO_2, the initial content of inactivated PSII was much lower as compared with that under 400 μatm pCO_2, again showing that high CO_2 enabled better clearance of inactivated PSII.

4.2. Combined effects of light, temperature and pCO_2 on photoprotection

NPQ is commonly considered a photoprotection mechanism by dissipating excess excitation energy in the form of heat (Goss and Jakob, 2010; Demmig-Adams et al., 2014). After the upward light shift, NPQs in *T. weissflogii* increased with exposure time, showing the activation of sustained photoprotection mechanisms to function against excess light energy. The increase was larger with the addition of lincomycin, indicating that NPQs plays a more important role in

maintaining PSII activity or limiting photoinactivation when PSII repair is blocked by inhibition of protein synthesis. The diatoms induce NPQs when photoinactivation outruns removal of PsbA protein (Wu et al., 2012a). In this study, we found that higher pCO_2 provoked higher NPQs at a lower ratio of K_{pi} to K_{PsbA} when cells were less photo-inhibited. An increased NPQ was also found in *Skeletonema costatum* and *Phaeodactylum tricornutum* grown at higher pCO_2 when exposed to high light (Gao et al., 2012). Algal CO_2 concentrating mechanisms are commonly down-regulated by increased CO_2 (Raven et al., 2017), which may lower algal capacity to rapidly drain excess electrons in the Calvin cycle during short-term high light exposure (Rost et al., 2006). This could lead to a lower photochemical capability to cope with high light (Ihnken et al., 2011) and may explain the high NPQs at a lower ratio of K_{pi} to K_{PsbA} for the higher pCO_2 treatment in the present study. On the other hand, the higher pCO_2 increased PsbA removal. Therefore, the negligible net effect of higher pCO_2 on the PSII quantum yield (F_V/F_M) after 120-min high light exposure could be a compromise between the negative and positive aspects.

Apart from NPQ, diatoms usually have an antioxidant network to act against environmental stressor (Drábková et al., 2007; Li et al., 2015; Smerilli et al., 2017). In the present study, high light exposure stimulated the synthesis of SOD and CAT in *T. weissflogii* grown under all conditions, suggesting the protective response of cells to high light stress. Particularly, cells growth at the higher temperature produced higher initial activities of SOD and CAT, followed by greater induction of SOD and CAT upon the upward light shift at the higher temperature, indicating that the higher temperature triggered additional detoxification processes to help protect PSII repair against ROS. Higher temperature also resulted in up-regulation of photo-protective gene LhcSR in green algae (Dong et al., 2012). The induced synthesis of SOD and CAT by the higher light and temperature may partially explain the higher K_{rec} compared to K_{psbA} (Fig. 5C).

Contrast to light and temperature, pCO_2 did not affect the amount of SOD or CAT in *T. weissflogii.* The ignorable effect of elevated pCO_2 on SOD and CAT was also reported in the diatom *Phaeodactylum tricornutum* (Li et al., 2015). This may indicate the less sensitivity of diatoms' antioxidant system to ocean acidification.

5. Conclusions

To predict future marine primary productivity and ecosystem functioning under the context of climate change, combined effects of primary climate variables and local stressors need to be considered. In this study, the interactive effects of ocean warming and acidification on PSII photoinactivation, repair and protection in the diatom *T. weissflogii* experiencing dynamic light were investigated for the first time. Our findings indicate that ocean warming will increase *T. weissflogii's* photoinactivation when it suffers a high light challenge. Meanwhile, ocean acidification could help alleviate the negative effect of ocean warming through increasing the PsbA removal rate. Although ocean warming and high light could stimulate ROS detoxification enzyme activity in *T. weissflogii,* it is not enough to fully offset the damage caused by high temperature combined with high light exposure, leading to net photoinactivation for *T. weissflogii.* Whether the observed interactive effects of ocean warming and acidification are unique for *T. weissflogii* or are widespread among phytoplankton taxa remains to be known.

Acknowledgements

This research was supported by the National Natural Science Foundation of China (Nos. 31270452; 91647207; 41376129 and 41476097), the Research Project of Chinese Ministry of Education (No. 213026A), the Natural Science Foundation of Hubei Province (2014CFB607), the Jiangsu Planned Projects for Postdoctoral Research Funds (1701003A), the Science and Technology Bureau of Lianyungang (SH1606), the Science Foundation of Huaihai Institute of Technology (Z2016007), the Priority Academic Program Development of Jiangsu Higher Education Institutions of China, and the Canada Research Chairs (DC).

References

Aro, E.-M., McCaffery, S., Anderson, J.M., 1993. Photoinhibition and D1 protein degradation in peas acclimated to different growth irradiances. Plant Physiol. 103, 835–843.
Behrenfeld, M.J., O'Malley, R.T., Siegel, D.A., Mcclain, C.R., Sarmiento, J.L., Feldma n, G.C., Milligan, A.J., Falkowski, P.G., Letelier, R.M., Boss, E.S., 2006. Climate-driven trends in contemporary ocean productivity. Nature 444, 752–755.
Brown, C.M., MacKinnon, J.D., Cockshutt, A.M., Villareal, T.A., Campbell, D.A., 2008. Flux capacities and acclimation costs in *Trichodesmium* from the Gulf of Mexico. Mar. Biol. 154, 413–422.
Campbell, D.A., Tyystjärvi, E., 2012. Parameterization of photosystem II photoinactivation and repair. BBA-Bioenergetics 1817, 258–265.
Campbell, D.A., Hossain, Z., Cockshutt, A.M., Zhaxybayeva, O., Wu, H., Li, G., 2013. Photosystem II protein clearance and FtsH function in the diatom *Thalassiosira pseudonana*. Photosynth. Res. 115, 43–54.
Demmig-Adams, B., Garab, G., Adams, W.W., Govindjee, 2014. Non-Photochemical Quenching and Energy Dissipation in Plants, Algae and Cyanobacteria. Springer, Netherlands.
Dong, M., Zhang, X., Zhuang, Z., Zou, J., Ye, N., Xu, D., Mou, S., Liang, C., Wang, W., 2012. Characterization of the LhcSR gene under light and temperature stress in the green alga *Ulva linza*. Plant Mol. Boil. Rep. 30, 10–16.
Drábková, M., Admiraal, W., Marsálek, B., 2007. Combined exposure to hydrogen peroxide and light-selective effects on cyanobacteria green algae, and diatoms. Environ. Sci. Technol. 41, 309–314.
Dubinsky, Z., Stambler, N., MacIntyre, H., Berman, T., Frank, I.B., 2009. Photoacclimation processes in phytoplankton: mechanisms, consequences, and applications. Aquat. Microb. Ecol. 56, 163–176.
Edelman, M., Mattoo, A.K., 2008. D1-protein dynamics in photosystem II: the lingering enigma. Photosynth. Res. 98, 609–620.
Falkowski, P., 2012. Ocean science: the power of plankton. Nature 483, 17–20.
Field, C.B., Behrenfeld, M.J., Randerson, J.T., Falkowski, P., 1998. Primary production of the biosphere: integrating terrestrial and oceanic components. Science 281, 237–240.
Gao, G., Gao, K., Giordano, M., 2009. Responses to solar UV radiation of the diatom *Skeletonema costatum* (Bacillariophyceae) grown at different Zn^{2+} concentrations. J. Phycol. 45, 119–129.
Gao, K., Xu, J., Gao, G., Li, Y., Hutchins, D.A., Huang, B., Wang, L., Zheng, Y., Jin, P., Cai, X., 2012. Rising CO_2 and increased light exposure synergistically reduce marine primary productivity. Nat. Clim. Change 2, 519–523.
Gao, G., Xia, J., Yu, J., Zeng, X., 2017a. Physiological response of a red tide alga (*Skeletonema costatum*) to nitrate enrichment, with special reference to inorganic carbon acquisition. Mar. Environ. Res. http://dx.doi.org/10.1016/j.marenvres.2017.11.003.
Gao, G., Jin, P., Liu, N., Li, F., Tong, S., Hutchins, D.A., Gao, K., 2017b. The acclimation process of phytoplankton biomass, carbon fixation and respiration to the combined effects of elevated temperature and pCO_2 in the northern South China Sea. Mar. Pollut. Bull. 118, 213–220.
Giovagnetti, V., Ruban, A.V., 2017. Detachment of the fucoxanthin chlorophyll a/c binding protein (FCP) antenna is not involved in the acclimative regulation of photoprotection in the pennate diatom *Phaeodactylum tricornutum*. BBA-Bioenergetics 1858, 218–230.
Goss, R., Jakob, T., 2010. Regulation and function of xanthophyll cycle-dependent photoprotection in algae. Photosynth. Res. 106, 103–122.
Guillard, R.R., Ryther, J.H., 1962. Studies of marine planktonic diatoms. I. *Cyclotella nana* hustedt, and *Detonula confervacea* (cleve) gran. Can. J. Microbiol. 8, 229–239.
Hoeghguldberg, O., Bruno, J.F., 2010. The impact of climate change on the world's marine ecosystems. Science 328, 1523–1528.
Hoppe, C.J., Holtz, L.M., Trimborn, S., Rost, B., 2015. Ocean acidification decreases the light-use efficiency in an Antarctic diatom under dynamic but not constant light. New Phytol. 207, 159–171.
IPCC, 2013. Climate change 2013: The physical science basis. In: Stocker, T.F., Qin, D., Plattner, G.-K., Tignor, M., Allen, S.K., Boschung, J., Nauels, A., Xia, Y., Bex, V., Midgley, P.M. (Eds.), Working Group I Contribution to the Fifth Assessment Report of the Intergovernmental Panel on Climate Change. Cambridge Univ Press, New York, pp. 6–10.
Ihnken, S., Roberts, S., Beardall, J., 2011. Differential responses of growth and photosynthesis in the marine diatom *Chaetoceros muelleri* to CO_2 and light availability. Phycologia 50, 182–193.
Jin, P., Gao, G., Liu, X., Li, F., Tong, S., Ding, J., Zhong, Z., Liu, N., Gao, K., 2016. Contrasting photophysiological characteristics of phytoplankton assemblages in the Northern South China Sea. PLoS One 11, e0153555.
Key, T., Mccarthy, A., Campbell, D.A., Six, C., Roy, S., Finkel, Z.V., 2010. Cell size trade-offs govern light exploitation strategies in marine phytoplankton. Environ. Microbiol. 12, 95–104.
Kok, B., 1956. On the inhibition of photosynthesis by intense light. B.B.A. 21, 234–244.
Komenda, J., Sobotka, R., Nixon, P.J., 2012. Assembling and maintaining the Photosystem II complex in chloroplasts and cyanobacteria. Curr. Opin. Plant Biol. 15, 245–251.
Lavaud, J., Lepetit, B., 2013. An explanation for the inter-species variability of the photoprotective non-photochemical chlorophyll fluorescence quenching in diatoms.

BBA-Bioenergetics 1827, 294–302.
Lavaud, J., Rousseau, B., Etienne, A.L., 2004. General features of photoprotection by energy dissipation in planktonic diatoms (Bacillariophyceae). J. Phycol. 40, 130–137.
Leblanc, K., Arístegui, J., Kopczynska, E., Marshall, H., Peloquin, J., Piontkovski, S., Poulton, A., Quéguiner, B., Schiebel, R., Shipe, R., 2012. A global diatom database–abundance, biovolume and biomass in the world ocean. Earth Syst. Sci. Data 4, 149–165.
Li, G., Campbell, D.A., 2013. Rising CO_2 interacts with growth light and growth rate to alter photosystem II photoinactivation of the coastal diatom *Thalassiosira pseudonana*. PLoS One 8, e55562.
Li, W., Gao, K., Beardall, J., 2015. Nitrate limitation and ocean acidification interact with UV-B to reduce photosynthetic performance in the diatom *Phaeodactylum tricornutum*. Biogeosciences 12, 2383–2393.
Macintyre, H.L., Kana, T.M., Geider, R.J., 2000. The effect of water motion on short-term rates of photosynthesis by marine phytoplankton. Trends Plant Sci. 5, 12–17.
Mathur, S., Agrawal, D., Jajoo, A., 2014. Photosynthesis: response to high temperature stress. J. Photechnol. Photobiol. B 137, 116–126.
McCarthy, A., Rogers, S.P., Duffy, S.J., Campbell, D.A., 2012. Elevated carbon dioxide differentially alters the photophysiology of *Thalassiosira pseudonana* (Bacillariophyceae) and *Emiliania huxleyi* (Haptophyta). J. Phycol. 48, 635–646.
Meehl, G., Stocker, T., Collins, W., 2007. Global climate projections. In: Solomon, S., Qin, D., Manning, M., Chen, Z., Marquis, M., Averyt, K., Tignor, M., Miller, H. (Eds.), Climate Change 2007: The Physical Science Basis. Contribution of Working Group I to the Fourth 16 Assessment Report of the Intergovernmental Panel on Climate Change. Cambridge University Press, Cambridge, UK, pp. 747–845.
Morel, F.M.M., Rueter, J.G., Anderson, D.M., Rrl, G., 1979. Aquil: a chemically defined phytoplankton culture medium for trace metal studies. J. Phycol. 15, 135–141.
Morris, E.P., Kromkamp, J.C., 2003. Influence of temperature on the relationship between oxygen-and fluorescence-based estimates of photosynthetic parameters in a marine benthic diatom (*Cylindrotheca closterium*). Eur. J. Phycol. 38, 133–142.
Mostofa, K.M., 2016. Reviews and syntheses: ocean acidification and its potential impacts on marine ecosystems. Biogeosciences 13, 1767–1786.
Murata, N., Takahashi, S., Nishiyama, Y., Allakhverdiev, S.I., 2007. Photoinhibition of photosystem II under environmental stress. B.B.A. 1767, 414–421.
NOAA, 2017. https://www.co2.earth/. USA.
Nagao, R., Tomo, T., Noguchi, E., Suzuki, T., Okumura, A., Narikawa, R., Enami, I., Ikeuchi, M., 2012. Proteases are associated with a minor fucoxanthin chlorophyll a/c-binding protein from the diatom, *Chaetoceros gracilis*. BBA-Bioenergetics 1817, 2110–2117.
Nelson, D.M., Tréguer, P., Brzezinski, M.A., Leynaert, A., Quéguiner, B., 1995. Production and dissolution of biogenic silica in the ocean Revised global estimates, comparison with regional data and relationship to biogenic sedimentation. Global Biogeochem. Cy. 9, 359–372.
Ni, G., Zimbalatti, G., Murphy, C.D., Barnett, A.B., Arsenault, C.M., Li, G., Cockshutt, A.M., Campbell, D.A., 2017. Arctic Micromonas uses protein pools and non-photochemical quenching to cope with temperature restrictions on Photosystem II protein turnover. Photosynth. Res. 131, 203–220.
Nishiyama, Y., Murata, N., 2014. Revised scheme for the mechanism of photoinhibition and its application to enhance the abiotic stress tolerance of the photosynthetic machinery. Appl. Microbiol. Biotechnol. 98, 8777–8796.
Nishiyama, Y., Allakhverdiev, S.I., Murata, N., 2006. A new paradigm for the action of reactive oxygen species in the photoinhibition of photosystem II. B.B.A 1757, 742–749.
Nixon, P.J., Michoux, F., Yu, J., Boehm, M., Komenda, J., 2010. Recent advances in understanding the assembly and repair of photosystem II. Ann. Bot. 106, 1–16.
Pierrot, D., Lewis, E., Wallace, D.W.R., 2006. MS Excel program developed for CO_2 system calculations. ORNL/CDIAC-105a. Carbon Dioxide Information Analysis Center, Oak Ridge National Laboratory, US Department of Energy, Oak Ridge, Tennessee.
Poll, W., Kulk, G., Timmermans, K., Brussaard, C., Woerd, H., Kehoe, M., Mojica, K., Visser, R., Rozema, P., Buma, A., 2013. Phytoplankton chlorophyll a biomass, composition, and productivity along a temperature and stratification gradient in the northeast Atlantic Ocean. Biogeosciences 10, 4227–4240.
Raven, J.A., Beardall, J., Sánchez-Baracaldo, P., 2017. The possible evolution, and future, of CO_2-concentrating mechanisms. J. Exp. Bot. http://dx.doi.org/10.1093/jxb/erx110.
Rost, B., Riebesell, U., Sültemeyer, D., 2006. Carbon acquisition of marine phytoplankton: effect of the photoperiodic length. Limnol. Oceanogr. 51, 12–20.
Shi, Q., Xiahou, W., Wu, H., 2016. Photosynthetic responses of the marine diatom *Thalassiosira pseudonana* to CO_2-induced seawater acidification. Hydrobiologia 361–369.
Six, C., Sherrard, R., Lionard, M., Roy, S., Campbell, D.A., 2009. Photosystem II and pigment dynamics among ecotypes of the green alga *Ostreococcus*. Plant Physiol. 151, 379–390.
Smerilli, A., Orefice, I., Corato, F., Gavalás, O.A., Ruban, A.V., Brunet, C., 2017. Photoprotective and antioxidant responses to light spectrum and intensity variations in the coastal diatom *Skeletonema marinoi*. Environ. Microbiol. 19, 611–627.
Sobrino, C., Neale, P.J., Lubián, L.M., 2005. Interaction of UV radiation and inorganic carbon supply in the inhibition of photosynthesis: spectral and temporal responses of two marine picoplankters. Photochem. Photobiol. 81, 384–393.
Sobrino, C., Ward, M.L., Neale, P.J., 2008. Acclimation to elevated carbon dioxide and ultraviolet radiation in the diatom *Thalassiosira pseudonana* Effects on growth, photosynthesis, and spectral sensitivity of photoinhibition. Limnol. Oceanogr. 53, 350.
Tyystjärvi, E., Aro, E.-M., 1996. The rate constant of photoinhibition, measured in lincomycin-treated leaves, is directly proportional to light intensity. Proc. Natl. Acad. Sci. U. S. A 93, 2213–2218.
van de Poll, W.H., van Leeuwe, M.A., Roggeveld, J., Buma, A.G.J., 2005. Nutrient limitation and high irradiance acclimation reduce PAR and UV-induced viability loss in the Antarctic diatom *Chaetoceros brevis* (Bacillariophyceae). J. Phycol. 41, 840–850.
Wang, M., Wang, G., 2010. Oxidative damage effects in the copepod *Tigriopus japonicus* Mori experimentally exposed to nickel. Ecotoxicology 19, 273–284.
Wu, H., Cockshutt, A.M., Mccarthy, A., Campbell, D.A., 2011. Distinctive photosystem II photoinactivation and protein dynamics in marine diatoms. Plant Physiol. 156, 2184–2195.
Wu, H., Roy, S., Alami, M., Green, B.R., Campbell, D.A., 2012a. Photosystem II photoinactivation, repair, and protection in marine centric diatoms. Plant Physiol. 160, 464–476.
Wu, X., Gao, G., Giordano, M., Gao, K., 2012b. Growth and photosynthesis of a diatom grown under elevated CO_2 in the presence of solar UV radiation. Fund. Appl. Limnol. 180, 279–290.
Xu, X., Liu, J., Shi, Q., Mei, H., Zhao, Y., Wu, H., 2016. Ocean warming alters photosynthetic responses of diatom *Phaeodactylum tricornutum* to fluctuating irradiance. Phycologia 55, 126–133.
Xu, Z., Gao, G., Xu, J., Wu, H., 2017. Physiological response of a golden tide alga (*Sargassum muticum*) to the interaction of ocean acidification and phosphorus enrichment. Biogeosciences 14, 671–681.
Yun, M.S., Lee, S.H., Chung, I.K., 2010. Photosynthetic activity of benthic diatoms in response to different temperatures. J. Appl. Phycol. 22, 559–562.